MODEL OF LATTICE DYNAMICS FOR BISMUTH

By A. Czachor*, A. Rajca** J. Sosnowski* and A. Pindor**

Institute of Nuclear Research, Świerk*

Institute of Experimental Physics, Warsaw University**

(Received February 8, 1972)

The five-neighbours, Born-von Karman model of the lattice dynamics of bismuth is developed. The model allows a semi-quantitative description of the experimental phonon data to be made. Computation of a frequency spectrum for bismuth has proved the existence of a frequency gap $\sim 1.8 \cdot 10^{12}$ rad/s (~ 1.2 meV) in the spectrum, which separates the acoustic and optical frequency bands.

Besides the model, general expressions for the elements of dynamical matrix and for elastic constants, taking into account the space group symmetry for the bismuth structure, are derived.

1. Introduction

Bismuth is a semi-metal, belonging to the V group of the periodic table. It crystallizes in the trigonal system, with two atoms in the primitive cell. The structure of Bi is very close to the simple cubic structure. Its space group $R\bar{3}m$ (D_{3d}^5) is symmorphic.

Due to the valency $Z = 5$ of bismuth, one has to construct a large zone to confine its 10 electrons per primitive cell [1]. There exists rather strong experimental evidence that the conduction band elipsoids are centered at points L, whereas the valence band elipsoids are centered at points T of the Brillouin zone [2]. A rather complete information on the electronic properties of Bi may be found in [3]. The lattice dynamics of Bi have been investigated by Yarnell *et al.* [4], Smith [5] and Macfarlane [17], mainly at 75°K, and by Sosnowski *et al.* [6] at room temperatures, using the neutron inelastic, coherent scattering method.

There are only a few theoretical treatments of the lattice dynamics for bismuth, all within the framework of the Born-von Karman theory. One has to mention here the

* Address: Instytut Badań Jądrowych, Świerk k.Otwocka, Poland.

** Address: Instytut Fizyki Doświadczalnej, Uniwersytet Warszawski, Hoża 69, 00-682 Warszawa, Poland.

two-neighbours model of Fouret [7], the one-dimensional chain model of Yarnell *et al.* [4] and the four-neighbours models used by Brovman [8] and Smith [5], who have also carried out the group-theoretical analysis and classification of phonon modes for this structure. These authors have obtained only a qualitative agreement with experiment, with the exception of Yarnell *et al.*, whose model is, however, applicable only for the trigonal direction phonon modes. For antimony, which has the same structure, the nine-neighbours model has recently been proposed [18].

In the present paper we propose the model for bismuth, which is more satisfactory than models quoted above. It is the five-neighbours Born-von Karman model. Contrary to other models it is, in principle, consistent with all the elastic constants data. Due to its simplicity, it can be also used within the least-squares fitting scheme with a reasonable computation labour. On the basis of the model, the frequency spectrum for bismuth has been computed.

Besides, we present general formulas for the elements of dynamical matrix and elastic constants for the bismuth structure, derived assuming unlimited number of interacting -neighbours. All information about the symmetry of Bi is already contained in these formulas.

2. *Dynamical matrix and the symmetry of bismuth*

The dynamical matrix of the Born-von Karman (BK) theory of lattice vibrations may be written as follows [9]:

$$D_{\alpha\beta}(\vec{q}|bb') = \frac{1}{\sqrt{M_b M_{b'}}} \sum_{l} \Phi_{\alpha\beta}\begin{pmatrix} l \\ bb' \end{pmatrix} \cdot \exp\left[-i\vec{q}\cdot\vec{r}\begin{pmatrix} l \\ bb' \end{pmatrix}\right]. \tag{1}$$

where $\vec{r}\begin{pmatrix} l \\ bb' \end{pmatrix} = \vec{l}+\vec{b}-\vec{b}'$, $\vec{l}$ is a lattice vector and M_b is the mass of atom in the position $\vec{b}$ in the primitive cell. $\Phi_{\alpha\beta}(\vec{r})$ is a force constant, describing a coupling between two atoms connected by the structure vector $\vec{r}$. The frequencies (squared) for a system are given as eigenvalues of the dynamical matrix (1). Force constants fulfil, among others, the following relations [9]

$$\Phi_{\alpha\beta}\begin{pmatrix} l \\ bb' \end{pmatrix} = \Phi_{\beta\alpha}\begin{pmatrix} -l \\ b'b \end{pmatrix}, \quad \Phi_{\alpha\beta}\begin{pmatrix} 0 \\ bb \end{pmatrix} = -\sum_{lb'}{}' \Phi_{\alpha\beta}\begin{pmatrix} l \\ bb' \end{pmatrix}. \tag{2}$$

Symmetry of a structure can lead to certain simplification of the general form of the force constants matrix. Let us define the coordination sphere group for a sublattice $\vec{b}$ of a given structure, as the point group of all rotations (proper or improper) around the atom at the position $\vec{b}$ in a primitive cell [19]. It is the subgroup of the point group for this structure. By applying the operations of the coordination sphere group to a vector joining a given atom with its neighbour one obtains a set of vectors connecting the atom with all its neighbours belonging to the same coordination sphere.

Now, if T is any symmetry operation of the space group of a structure considered, transforming the structure vector $\vec{r}$ into $\vec{r}'$

$$T\vec{r} = \vec{r}' \tag{3}$$

then corresponding force matrices are connected by the similarity transformation [10]:

$$\Phi(\vec{r}') = T \cdot \Phi(\vec{r}) \cdot T^{-1}. \tag{4}$$

It follows, that all the force matrices of the coordination sphere atoms can be expressed in terms of one of them. Besides, if the structure vector $\vec{r}$ lies on a mirror plane or along an axis of rotation, then relation (4) introduces usually certain simplifications of the general form of $\Phi(\vec{r})$.

Fig. 1 shows the projection of the bismuth structure on the mirror plane. Full circles and squares represent atoms situated exactly in the plane or atoms equivalent to them

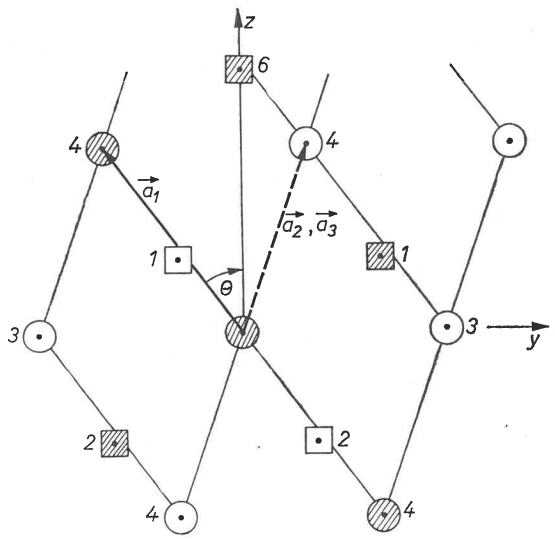

Fig. 1. Projection of the bismuth structure on the mirror plane. Circles — atoms of the "first" sublattice. Squares — atoms of the "second" sublattice. Hatched circles and squares symbolize atoms situated on the mirror plane or equivalent ones. Open circles and squares — atoms below or above this plane

through a lattice translation. Empty circles and squares represent atoms not having this property. Consequently, the primitive translation vector $\vec{a}_1$ lies in the mirror plane, whereas $\vec{a}_2$ and $\vec{a}_3$ are oblique to it. The Cartesian, right-hand coordinate system is chosen so, that the z-axis goes along the trigonal axis and the x-axis is perpendicular to the mirror plane $z-y$.

Parameters of the Bi structure are given in Table II. For the simple cubic structure there would be $u = 1/4$ (*i. e.* the squares in Fig. 1 situated exactly midway between the corresponding pairs of circles) and $\alpha = 60°$ (where $\sin\theta = 2/\sqrt{3} \cdot \sin(\alpha/2)$; it follows, that the structure of bismuth is indeed very close to the simple cubic structure.

The coordination sphere group for Bi is C_{3v}, consisting of 6 operations. They can be generated from the following two:

$$T(C_3) = \begin{bmatrix} -\frac{1}{2} & -\frac{\sqrt{3}}{2} & 0 \\ \frac{\sqrt{3}}{2} & -\frac{1}{2} & 0 \\ 0 & 0 & 1 \end{bmatrix}, \quad T(C_s) = \begin{bmatrix} -1 & 0 & 0 \\ 0 & 1 & 0 \\ 0 & 0 & 1 \end{bmatrix}. \tag{5}$$

With the help of (4) one can perform in (1) the partial summations within coordination spheres (a more detailed presentation of such a procedure may be found in the paper [11] for hexagonal, close-packed structure). Resulting formulas for the elements of dynamical matrix are given in the Appendix A. The sublattice I can be transferred into the sublattice II by performing the rotation around the binary axis (this operation of the space group does not belong to the coordination sphere group). It leads to the following relation

$$\Phi_{\alpha\beta}\begin{pmatrix} l \\ 12 \end{pmatrix} = \Phi_{\beta\alpha}\begin{pmatrix} l \\ 12 \end{pmatrix}. \tag{6}$$

It is convenient to use the following notation for the force matrices

$$\Phi_{\alpha\beta}\begin{pmatrix} l \\ 11 \end{pmatrix} = \begin{pmatrix} a & f & e \\ k & b & d \\ l & m & g \end{pmatrix}, \quad \Phi_{\alpha\beta}\begin{pmatrix} l \\ 12 \end{pmatrix} = \begin{pmatrix} A & F & E \\ F & B & D \\ E & D & G \end{pmatrix}. \tag{7}$$

The standard, long wave procedure [9] leads to general expressions for the elastic constants and invariance and Huang conditions. They are given in the Appendix A.

3. Description of the model

The Bi structure has rather low symmetry as compared with other monoatomic crystal structures. As a result the expressions for all the elastic constants and for most of the phonon frequencies are non-linear in force constants. The low symmetry results also in a small number of atoms in every coordination sphere. Hence the number of independent force constants can be quite high, even if the coupling with only few nearest neighbours is assumed. The construction of the soluble Born-von Karman model which allows for interactions with more than 4 nearest neighbours and which is consistent with all the elastic constants meets with serious difficulties.

In this paper we present the model in which every atom couples with its neighbours belonging to five coordination spheres, as shown in Table I. The matrices of interaction with first and second coordination sphere atoms have the most general form allowed by the symmetry. The force matrix Φ_3 for the $(\sqrt{3}\tau, 0, 0)$ atom follows from assuming the interaction potential of a cylindrical symmetry. Matrix Φ_4 is assumed to represent axial

forces (derivable from radially symmetric potential of interaction). Also by assumption, the corresponding coordination sphere consists of 6 atoms, although they are not all equivalent with respect to the C_{3v} group operations. The interaction with the nearest neigh-

TABLE I

The Model

Position of the representative atom of a coordination sphere	Force matrix Φ_n	Weight factor ϱ_n
$\begin{pmatrix} 0 \\ \tau \\ (6u-1)\varrho \end{pmatrix}$	$\begin{pmatrix} A_1 & 0 & 0 \\ 0 & B_1 & D_1 \\ 0 & D_1 & G_1 \end{pmatrix}$	$\frac{1}{2}$
$\begin{pmatrix} 0 \\ -\tau \\ (6u-2)\varrho \end{pmatrix}$	$\begin{pmatrix} A_2 & 0 & 0 \\ 0 & B_2 & D_2 \\ 0 & D_2 & G_2 \end{pmatrix}$	$\frac{1}{2}$
$\begin{pmatrix} \sqrt{3}\,\tau \\ 0 \\ 0 \end{pmatrix}$	$\begin{pmatrix} a_3 & 0 & 0 \\ 0 & b_3 & 0 \\ 0 & 0 & g_3 \end{pmatrix}$	1
$\begin{pmatrix} 0 \\ -\tau \\ \varrho \end{pmatrix}$	$\begin{pmatrix} a_4 & 0 & 0 \\ 0 & b_4 & d_4 \\ 0 & d_4 & g_4 \end{pmatrix}$	1
$\begin{pmatrix} 0 \\ 0 \\ 6u\varrho \end{pmatrix}$	$\begin{pmatrix} A_6 & 0 & 0 \\ 0 & A_6 & 0 \\ 0 & 0 & G_6 \end{pmatrix}$	$\frac{1}{6}$

$$\tau = a \sin\theta,\ \varrho = a\cos\theta,\ \sin\theta \equiv \frac{2}{\sqrt{3}} \sin\left(\frac{\alpha}{2}\right)$$

$$a_4 = t_4,\ b_4 = \sin^2\theta \cdot l_4 + t_4,\ g_4 = \cos^2\theta \cdot l_4 + t_4$$

$$d_4 = -\sin\theta\cos\theta \cdot l_4$$

bour in the direction of the trigonal axis is described by the matrix Φ_6, which is only symmetry restricted.

We have also tried to construct models including interactions with the fifth neighbours (coordination sphere of the $(0, -2\tau, (6u-1)\varrho)$ atom) and have found that it increases considerably the mathematical complexity of the problem, but gives no great improvement in the quality of the final result. At the same time, it was crucial, for the purpose of fitting the calculated and experimental phonon dispersion curves for the direction $\Gamma-T$ (Fig. 2), to include in the model interaction with the $(0,0,6u\varrho)$ atom. The model presented in Table I is probably the most general one, for which one can determine the force constants with no more difficulties than solving the quadratic equations.

The elastic constants and certain phonon frequencies for the points Γ, T, L and X of the Brillouin zone have been expressed in terms of the force constants of the model. Besides, the rotational invariance condition and the Huang conditions have been written,

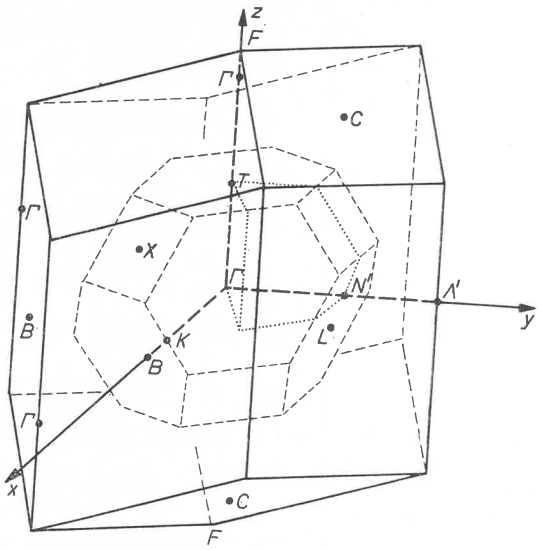

Fig. 2. Jones zone, Brillouin zone and the irreducible part of the Brillouin zone for the bismuth structure

as it is shown in the Appendix B (Eqs (B13), (B14), (B15). These are 19 equations, from which one has to find 15 unknown force constants of the model. We have solved this problem in two ways:

1. Algebraic approach. Equations (B16), (B17), (B18) and (B19) have been omitted and the system of remaining 15 equations solved. It means, that the algebraic approach (AA)

TABLE II

Parameters of the Bi structure at 298°K [15]

$a = 4.7458$ Å
$\alpha = 57°13'48''$
$u = 0.23389$

TABLE III

Elastic constants of Bi at room temperature [16]

$[10^{10}$ dyn $\cdot$ cm$^{-2}]$

$c_{11} =$	63.7 ± 0.2
$c_{12} =$	24.9 ± 0.2
$c_{13} =$	24.7 ± 0.2
$c_{14} =$	-7.17 ± 0.04 [1]
$c_{33} =$	38.2 ± 0.2
$c_{44} =$	11.23 ± 0.04
$c_{66} =$	19.41 ± 0.06

[1] For our choice of the system of coordinates c_{14} is negative.

gives the solution consistent with all elastic constants and with phonon frequencies at points Γ and T. The occurrence of nonlinear equations in the system (B1)–(B15) leads to 4 independent and formally equivalent sets of force constants. However, for only one of them (Table IV) the acoustic and optical phonon branches for directions $\Gamma-L$ and $\Gamma-X$ do not cross, in accordance with experimental data. This set of force constants has been accepted. The corresponding, calculated phonon dispersion curves are shown in Fig. 3 (dashed lines). We notice the large discrepancy between experimental and calculated frequencies and, in particular, the occurrence of imaginary frequencies in the vicinity of point X.

2. The least squares fitting (LSF). The sum of squares of the differences between the left (e_i) and ringht (t_i) sides of equations (B1)–(B19) (Appendix B) was formed

$$Z = \sum_i \frac{(e_i - t_i)^2}{e_i^2} \tag{8}$$

and minimalized with respect to the force constants. In (8) the i-summation goes over equations (B1)–(B19). To assure the physical consistency of the model, the rotational invariance condition and Huang conditions (Eqs (B13), (B14) and (B15)) have been satisfied exactly. Also, as the difficulties in achieving the fit to the experimental data are connected mainly with the Φ_{xx} and Φ_{yy} force constants, certain equations involving only the Φ_{zz} force constants have been chosen to be satisfied exactly (Eqs (B5), (B7), (B11) and (B12)). In the process of minimalization Z changed from 1.1. to 0.3. The resulting set of force constants, corresponding to the AA set as the starting data, is given in Table IV. Fig. 3 shows the phonon dispersion curves calculated for the LSF set of force constants (point-dash lines). The fit between calculated and experimental curves is as a whole much better, than in the AA case. However, the values of elastic constants and phonon frequencies at Γ and T have been somewhat changed in the process of minimalization.

4. Phonon dispersion curves for bismuth

We show in Fig. 3 the room temperature experimental phonon curves, determined for directions $\Gamma-T$, $\Gamma-L$, $\Gamma-X$ and $\Gamma-N-A'-X$ by Sosnowski *et al.* [6], and for direction $\Gamma-T$ also by Yarnell *et al.* [4] and the 75°K data of Macfarlane [17] for direction $\Gamma-K-X$. There exist no experimental, room temperature data for this direction. However, for most of the phonons investigated in Bi, the room temperature phonon frequencies differ from those corresponding to 75°K by no more than 1% [4]. For this reason we treat the 75°K data as representative, within experimental error, for room temperatures, too.

For all the directions investigated the acoustic branches are well separated from optical ones. The acoustic branches for directions $\Gamma-X$ show large dispersion. The optical branches are relatively flat. It seems, that the highest frequency for bismuth corresponds to the branch A^1 ($\sim 2.1 \cdot 10^{13}$ rad/s). As a whole, phonon dispersion curves in Bi resemble the curves for some ionic crystals [12].

Fig. 3 presents also calculated phonon dispersion curves. The AA curves evidently

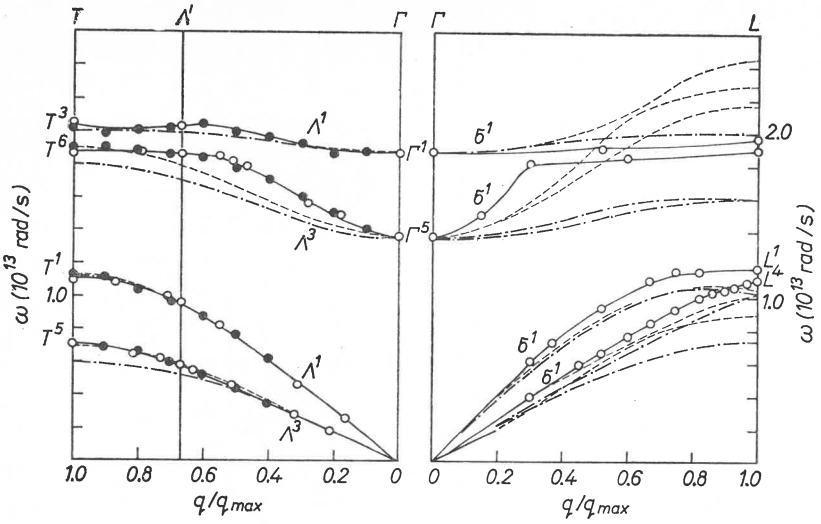
Γ
Λ'
Γ
Γ
L
T³
T⁶
T¹
T⁵
Λ¹
Λ³
Γ¹
Γ⁵
Δ¹
2.0
1.0
L¹
L⁴
ω (10¹³ rad/s)
1.0 0.8 0.6 0.4 0.2 0
0 0.2 0.4 0.6 0.8 1.0
q/q_max

a

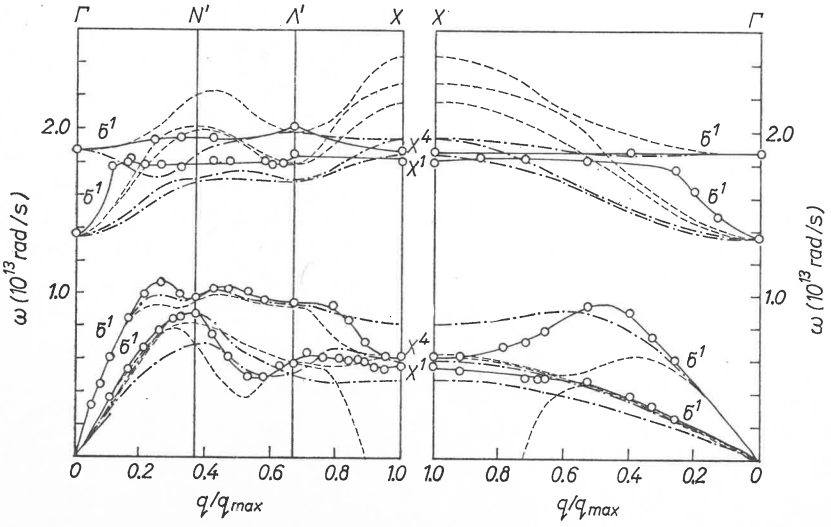
Γ
N'
Λ'
X
X
Γ
2.0
1.0
Δ¹
X⁴
X¹
ω (10¹³ rad/s)
0 0.2 0.4 0.6 0.8 1.0
1.0 0.8 0.6 0.4 0.2 0
q/q_max

b

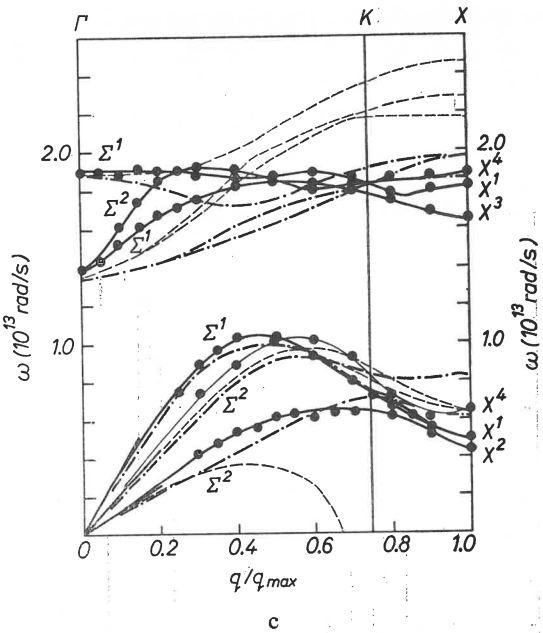

Fig. 3. Phonon dispersion curves for bismuth (a, b, c). Full lines — hand drawn through experimental point. Open circles — room temperature data of Sosnowski *et al.* [6]. Black circles — liquid nitrogen data of Yarnell *et al.* [4] and Macfarlane [17]. Dashed lines — phonon dispersion curves calculated basing on the AA force constants. Point-dash lines (.—.—.) — the curves calculated with the force constants of the LSF calculation scheme

cannot be accepted. The LSF curves show a semi-qualitative agreement with experimental data. The acoustic and optical frequency bands have proper widths, they are well separated. Optical branches are rather flat. Acoustic branches for the directions $\Gamma-X$ indeed show a large dispersion and two of the phonon frequencies at X ($\omega(X^2)$ is one of them) are very low.

However, the detailed behaviour of the experimental phonon curves, in particular the acoustic curves along directions $\Gamma-X$ and $\Gamma-K-X$ and optical branches for the direction $\Gamma-L$, is reproduced rather roughly. A better fit cannot be probably achieved within such a simple model.

5. *Frequency spectrum of bismuth*

The frequency spectrum was computed for the LSF case, using the perturbation sampling method [13]. The secular equation for the dynamical matrix was solved for a mesh of about 100 points distributed uniformly within irreducible part of the Brillouin zone (Fig. 2). The obtained eigenvectors were used to calculate approximate eigenfrequencies at 27 points distributed uniformly about every mesh point. Every frequency was given a weight, following from the symmetry considerations (1 for the internal points, less than 1 for the boundaries of the irreducible part of BZ, ex. 1/12 for point T). The

frequencies were then sorted into the frequency intervals 10^{12} rad/s. The frequency spectrum was set up by summing all the weights in every frequency interval. The GIER computer at INR Świerk was used for computations.

The calculated frequency spectrum is shown in Fig. 4. No attempt was made to use a denser mesh in order to obtain a fine structure of the spectrum, as, because of the short-

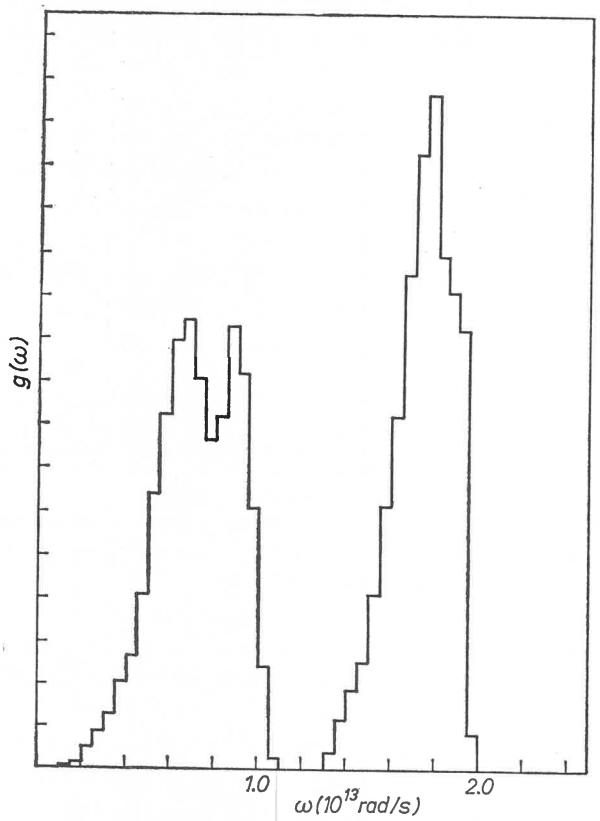

Fig. 4. The calculated phonon frequency spectrum for bismuth, based on the LSF force constants

comings of the model used, only main features of the spectrum could be considered to be reliable.

There is a gap in the calculated phonon spectrum of Bi, which separates the acoustic and optical bands of frequencies. It should be noted that the frequency distribution function, determined experimentally by Kotov *et al.* [14] shows indeed very low values in the corresponding region of frequencies.

It follows from the experiment and from the present calculations, that the frequency gap in bismuth ranges between the highest acoustic frequency for the direction $\Gamma-L$ and the optical frequency $\omega(\Gamma^5)$. Experimental figure for the gap's width at room temperature is $\omega(\Gamma^5)-\omega(L^1) \sim 1.8 \cdot 10^{12}$ rad/s ($\sim$ 1.2 meV). It is the first case, that the energy gap is found in the phonon spectrum of a monoatomic crystal.

6. Discussion

The AA version of the model, in spite of its formal advantages over the earlier models [5, 8] (the possibility of fitting simultaneously the phonon frequencies at Γ and T, and the elastic constants c_{33}, c_{44}) is unable to describe the experimental situation. Evidently, the atomic interactions are oversimplified in it. In fact, the fourier analysis of the trace of the dynamical matrix suggests, that at least nine nearest coordination spheres of neighbours should be incorporated into the model, to account for the observed shapes of phonon curves [17]. This would complicate the mathematics of the problem enormously.

For this reason, and for the interpolation purposes, we have made an effort to improve the description of the experimental situation within the five neighbours model. The least squares fitting allowed to achieve the semi-quantitative agreement with the experiment, so that the main features of experimental result are reproduced within the LSF version of the model.

There is a very strong coupling with the nearest neighbours in bismuth (Tr $\Phi_1 \gg$ Tr Φ_2). The relative smallness of A_1, if treated in terms of the ion-ion interaction potential $V(r)$ (depending on the distance only, so $A_1 \sim V(r)/r|_{r=|\vec{l}|}$) would mean, that a distance between nearest neighbours is close to the position of the minimum of $V(r)$. One cannot, however, expect, that interactions in bismuth have such a simple form. Evident domination of interactions with nearest neighbours suggests anisotropy of interactions and perhaps their directional, covalent character.

TABLE IV

Five-neighbours model of lattice dynamics for bismuth. Force constants [dyn cm^{-1}]

The AA set of force constants

	Φ_1	Φ_2	Φ_3	Φ_4	Φ_6
A	$9.4 \cdot 10^3$	$1.16 \cdot 10^4$	$-7.0 \cdot 10^3$	$-3.5 \cdot 10^3$	$3 \cdot 10^2$
B	$-3.81 \cdot 10^4$	$-4.4 \cdot 10^3$	$-2.8 \cdot 10^3$	$-3.0 \cdot 10^3$	$3 \cdot 10^2$
D	$-3.34 \cdot 10^4$	$-9.9 \cdot 10^3$	0	$-6 \cdot 10^2$	0
G	$-1.81 \cdot 10^4$	$-4.1 \cdot 10^3$	$-1.1 \cdot 10^3$	$-2.5 \cdot 10^3$	$5.2 \cdot 10^3$

The LSF set of force constants

	Φ_1	Φ_2	Φ_3	Φ_4	Φ_6
A	$2.3 \cdot 10^3$	$5.2 \cdot 10^3$	$-5.0 \cdot 10^3$	$-2.6 \cdot 10^3$	$4.5 \cdot 10^3$
B	$-2.94 \cdot 10^4$	$-2.0 \cdot 10^3$	$-3 \cdot 10^2$	$-2.6 \cdot 10^3$	$4.5 \cdot 10^3$
D	$-1.93 \cdot 10^4$	$-6.4 \cdot 10^3$	0	$1 \cdot 10^2$	0
G	$-1.81 \cdot 10^4$	$-4.1 \cdot 10^3$	$1.6 \cdot 10^3$	$-2.5 \cdot 10^3$	$5.2 \cdot 10^3$

Both A_6 and G_6 are positive (Table IV). Perhaps one should tie this fact with the easy cleavage plane occurring in Bi, which is perpendicular to the trigonal axis.

The present model (as well as the earlier ones [5, 8]) is unable to reproduce the complicated behaviour of experimental phonon curves in the vicinity of point X. Presumably the

low values of acoustic frequencies in this region reflect a certain instability tendency of this structure, which cannot be accounted for by such a simple model.

Although the deviation of the structure of bismuth from the simple cubic is rather small, it leads to a very large modification of the phonon spectrum, including the occurrence of the energy gap. In terms of force constants, the splitting between acoustic and optical frequencies at points T and L appears because diagonal force constants, describing the coupling with first and second nearest neighbours, differ (Table IV). Assuming for a while $\Phi_6 = 0$, one finds, that the splitting disappears, if $\Phi_1 = \Phi_2$ (see Appendix B, Eqs (B10) and (B12)), which occurs just in the case of undeformed, simple cubic structure. Splitting at point X exists for the cubic structure, too.

It is interesting to compare the temperature dependence of higher phonon frequencies with the temperature dependence of the sound velocities in bismuth. In the temperature range 75°K–300°K the higher photon frequencies (determined by neutron scattering) change by $\sim 1\%$ [4], whereas the sound velocities (determined by the ultrasonic method) change by about 5% [16]. This would suggest the temperature change of the long-range screening, possibly due to the temperature dependence of the energy spectrum of conduction electrons, resulting from interaction with phonons (*i.e.* the failure of the adiabatic approximation), or the temperature dependence of the bands population.

The occurence of the gap in the phonon spectrum of bismuth does not influence its thermodynamic properties drastically (phonons are bosons). Certain effects can, nevertheless, be expected, such as nonmonotonic behaviour of the temperature derivative of the lattice specific heat *vs* temperature.

APPENDIX A

Elements of dynamical matrix for the structure of bismuth

$$MD_{11}\begin{pmatrix}\vec{k}\\11\end{pmatrix} = \Phi_{11}\begin{pmatrix}0\\11\end{pmatrix} + 2\sum_n \varrho_n \{a_n \cos(x) e^{i(zy)} +$$

$$+ \tfrac{1}{4}(a_n + 3b_n + \sqrt{3}(f_n + k_n)) \cos(xy) e^{i(zxy)} +$$

$$+ \tfrac{1}{4}(a_n + 3b_n - \sqrt{3}(f_n + k_n)) \cos(yx) e^{i(zyx)}\}$$

$$MD_{22}\begin{pmatrix}\vec{k}\\11\end{pmatrix} = \Phi_{22}\begin{pmatrix}0\\11\end{pmatrix} + 2\sum_n \varrho_n \{b_n \cos(x) e^{i(zy)} +$$

$$+ \tfrac{1}{4}(3a_n + b_n - \sqrt{3}(f_n + k_n)) \cos(xy) e^{i(zxy)} +$$

$$+ \tfrac{1}{4}(3a_n + b_n + \sqrt{3}(f_n + k_n)) \cos(yx) e^{i(zyx)}\}$$

$$MD_{33}\begin{pmatrix}\vec{k}\\11\end{pmatrix} = \Phi_{33}\begin{pmatrix}0\\11\end{pmatrix} + 2\sum_n \varrho_n g_n \{\cos(x) e^{i(zy)} + \cos(xy) e^{i(zxy)} + \cos(yx) e^{i(zyx)}\}$$

$$MD_{12}\begin{pmatrix}\vec{k}\\11\end{pmatrix} = 2i\sum_n \varrho_n\{-f_n \sin(x)e^{i(zy)} +$$

$$+ \tfrac{1}{4}(\sqrt{3}(-a_n+b_n)+f_n-3k_n)\sin(xy)e^{i(zxy)} +$$

$$+ \tfrac{1}{4}(\sqrt{3}(a_n-b_n)+f_n-3k_n)\sin(yx)e^{i(zyx)}\}$$

$$MD_{13}\begin{pmatrix}\vec{k}\\11\end{pmatrix} = -2i\sum_n \varrho_n\{e_n \sin(x)e^{i(zy)} +$$

$$+ \tfrac{1}{2}(e_n+\sqrt{3}\,d_n)\sin(xy)e^{i(zxy)} +$$

$$+ \tfrac{1}{2}(e_n-\sqrt{3}\,d_n)\sin(yx)e^{i(zyx)}\}$$

$$MD_{23}\begin{pmatrix}\vec{k}\\11\end{pmatrix} = 2\sum_n \varrho_n\{d_n \cos(x)e^{i(zy)} +$$

$$+ \tfrac{1}{2}(\sqrt{3}\,e_n-d_n)\cos(xy)e^{i(zxy)} -$$

$$- \tfrac{1}{2}(\sqrt{3}\,e_n+d_n)\cos(yx)e^{i(zyx)}\}$$

$$D_{\beta\alpha}\begin{pmatrix}\vec{k}\\11\end{pmatrix} = D^*_{\alpha\beta}\begin{pmatrix}\vec{k}\\11\end{pmatrix}$$

notation:

$$(x) \equiv 2\pi k_x x_n \qquad (zy) \equiv -2\pi(k_y y_n + k_z z_n)$$

$$(xy) \equiv \pi k_x(x_n+\sqrt{3}\,y_n) \qquad (zxy) \equiv -2\pi(k_y(\sqrt{3}\,x_n-y_n)/2+k_z z_n)$$

$$(yx) \equiv \pi k_x(x_n-\sqrt{3}\,y_n) \qquad (zyx) \equiv -2\pi(-k_y(\sqrt{3}\,x_n+y_n)/2+k_z z_n)$$

The elements $D_{\alpha\beta}\begin{pmatrix}\vec{k}\\12\end{pmatrix}$ can be derived from $D_{\alpha\beta}\begin{pmatrix}\vec{k}\\11\end{pmatrix}$ by:

1. Omitting the first terms — $\Phi_{\alpha\alpha}\begin{pmatrix}0\\11\end{pmatrix}$, on the right, in $D_{\alpha\alpha}\begin{pmatrix}\vec{k}\\11\end{pmatrix}$.

2. Changing to capital letters for the force constants and position coordinates, and simultaneously substituting k by F, l by E and m by D.

In the above formulas one takes into account only one position vector for every coordination sphere, *i.e.*(x_n, y_n, z_n) or (X_N, Y_N, Z_N).

ϱ_n = 1/6 · number of atoms in the n-th coordination sphere.

The self-force matrix elements have the following form

$$\Phi_{11}\begin{pmatrix}0\\11\end{pmatrix} = \Phi_{22}\begin{pmatrix}0\\11\end{pmatrix} = -3\sum_n \varrho_n(a_n+b_n) - 3\sum_N \varrho_N(A_N+B_N)$$

$$\Phi_{33}\begin{pmatrix}0\\11\end{pmatrix} = -6\sum_n \varrho_n g_n - 6\sum_N \varrho_N G_N$$

Elastic constants for the structure of bismuth

The long-wave procedure allows one to express elastic constants in terms of force constants. These are rather cumbersome expressions for the bismuth structure. It is convenient to express first the elastic constants by the "square and round brackets" [9]:

$$C_{11} = [11, 11]+(11, 11)$$

$$C_{12} = 2[12, 12]-[22, 11]+(11, 22)$$

$$C_{13} = 2[13, 13]-[33, 11]+(11, 33)$$

$$C_{14} = 2[12, 13]-[23, 11]+(11, 23)$$

$$C_{33} = [33, 33]+(33, 33)$$

$$C_{44} = [22, 33]+(23, 23)$$

$$[11, 11] = -\frac{3}{4v_a}\{\sum \varrho_n[a_n(3x_n^2+y_n^2)+b_n(x_n^2+3y_n^2)]+\mathrm{CL}\}$$

$$(11, 11) = \frac{3}{4v_a}[\{\sum \varrho_n[x_n(f_n+k_n)+y_n(a_n-b_n)]+\mathrm{CL}\}^2/\sum \varrho_N(A_N+B_N)+$$

$$+2\{\sum \varrho_n(l_nx_n+m_ny_n)+\mathrm{CL}\}^2/\sum \varrho_N G_N]$$

$$[12, 12] = -\frac{3}{4v_a}\{\sum \varrho_n[2x_ny_n(f_n+k_n)+(a_n-b_n)(x_n^2-y_n^2)]+\mathrm{CL}\}$$

$$[22, 11] = -\frac{3}{4v_a}\{\sum \varrho_n[a_n(x_n^2+3y_n^2)+b_n(3x_n^2+y_n^2)]+\mathrm{CL}\}$$

$$(11, 22) = \frac{3}{4v_a}[2\{\sum \varrho_n[l_nx_n+m_ny_n]+\mathrm{CL}\}^2/\sum \varrho_N G_N-$$

$$-\{\sum \varrho_n[x_n(f_n+k_n)+y_n(a_n-b_n)\}^2/\sum \varrho_N(A_N+B_N)]$$

$$[13, 13] = -\frac{3}{v_a}\{\sum \varrho_n z_n[e_nx_n+d_ny_n]+\mathrm{CL}\}$$

$$[33, 11] = -\frac{3}{v_a}\{\sum \varrho_n g_n[x_n^2+y_n^2]+\mathrm{CL}\}$$

$$(11, 33) = \frac{3}{v_a}\{\sum \varrho_n[l_nx_n+m_ny_n]+\mathrm{CL}\}\{\sum \varrho_n z_n g_n+\mathrm{CL}\}/\sum \varrho_N G_N$$

$$[12, 13] = -\frac{3}{2v_a}\{\sum \varrho_n z_n[x_n(f_n+k_n)+y_n(a_n-b_n)]+\mathrm{CL}\}$$

$$[23, 11] = -\frac{3}{2v_a}\{\sum \varrho_n[2e_n x_n y_n + d_n(x_n^2 - y_n^2)] + \mathrm{CL}\}$$

$$(11, 23) = \frac{3}{2v_a}\{\sum \varrho_n[x_n(f_n + k_n) + y_n(a_n - b_n)] +$$

$$+\mathrm{CL}\}\{\sum \varrho_n z_n(a_n + b_n) + \mathrm{CL}\}/\sum \varrho_N(A_N + B_N)$$

$$[33, 33] = -\frac{6}{v_a}\{\sum \varrho_n g_n z_n^2 + \sum \varrho_N G_N Z_N^2\}$$

$$(33, 33) = \frac{6}{v_a}\{\sum \varrho_n g_n z_n + \sum \varrho_N G_N Z_N\}^2/\sum \varrho_N G_N$$

$$[22, 33] = -\frac{3}{v_a}\{\sum \varrho_n z_n^2(a_n + b_n) + \mathrm{CL}\}$$

$$(23, 23) = \frac{3}{v_a}\{\sum \varrho_n z_n(a_n + b_n) + \mathrm{CL}\}^2/\sum \varrho_N(A_N + B_N)$$

For brevity we use the symbol CL, which means: the same, but written in capital letters (with an obvious substitution, $k \to F$, $l \to E$, $m \to D$), ex. $\{\sum \varrho_n l_n x_n + \mathrm{CL}\}$ means $\{\sum \varrho_n l_n x_n + \sum \varrho_N E_N X_N\}$.

There exist additional conditions on the force constants, namely:

The condition expressing the rotational invariance of the crystal energy:

$$\sum \varrho_n z_n(a_n + b_n) + \mathrm{CL} = \sum \varrho_n(e_n x_n + d_n y_n) + \mathrm{CL}.$$

The Huang conditions for vanishing anisotropic stresses [9]:

$$\sum \varrho_n z_n[x_n(f_n + k_n) + y_n(a_n - b_n)] + \mathrm{CL} =$$

$$= \sum \varrho_n[m_n(x_n^2 - y_n^2) + 2l_n x_n y_n] + \mathrm{CL}$$

$$\sum \varrho_n z_n^2(a_n + b_n) + \mathrm{CL} = \sum \varrho_n g_n(x_n^2 + y_n^2) + \mathrm{CL}$$

$$\sum \varrho_n z_n[x_n(f_n + k_n) + y_n(a_n - b_n)] + \mathrm{CL} =$$

$$= \sum \varrho_n[d_n(x_n^2 - y_n^2) + 2e_n x_n y_n] + \mathrm{CL}$$

APPENDIX B

Elastic constants and some phonon frequencies expressed in terms of force constants of the model

$$C_{11} = -\frac{1}{4\sqrt{3}\,\varrho}[A_1 + 3B_1 + A_2 + 3B_2 + 18a_3 + 6b_3 + 2a_4 + 6b_4] +$$

$$+\frac{3}{4v_a}\left[\frac{U_2^2}{S_{AB}} + 2\frac{U_1^2}{S_G}\right] \qquad \text{(B1)}$$

$$C_{11}+C_{12}=\frac{1}{\sqrt{3}\,\varrho}\left[A_1-B_1+A_2-B_2-6a_3+6b_3+2a_4-2b_4\right]+\frac{3}{v_a}\frac{U_1^2}{S_G} \tag{B2}$$

$$C_{13}=\frac{1}{\sqrt{3}\,\varrho}\left[G_1+G_2+6g_3+2g_4-2\operatorname{ctg}\theta((6u-1)D_1+(2-6u)D_2-2d_4)\right]+$$

$$+\frac{3}{v_a}\frac{U_1U_3}{S_G} \tag{B3}$$

$$C_{14}=-\frac{1}{2\sqrt{3}\,\tau}\left[(6u-1)\,(A_1-B_1)+(2-6u)\,(A_2-B_2)-2a_4+2b_4\right]+$$

$$+\frac{3}{2v_a}\frac{U_1U_2}{S_{AB}} \tag{B4}$$

$$C_{33}=-\frac{2}{\sqrt{3}\,\tau}\operatorname{ctg}\theta\left[(6u-1)^2G_1+(2-6u)^2G_2+12u^2G_6+2g_4\right]+\frac{6}{v_a}\frac{U_3^2}{S_G} \tag{B5}$$

$$C_{44}=-\frac{\operatorname{ctg}\theta}{\sqrt{3}\,\tau}\left[(6u-1)^2(A_1+B_1)+(2-6u)_2^2(A_2+B_2)+24u^2A_6+2(a_4+b_4)\right]+$$

$$+\frac{3}{v_a}\frac{U_1^2}{S_{AB}} \tag{B6}$$

where

$$U_1\equiv\frac{\varrho}{2}\left[(6u-1)\,(A_1+B_1)-(2-6u)\,(A_2+B_2)+4uA_6\right]$$

$$U_2\equiv\frac{\tau}{2}\left[A_1-B_1-A_2+B_2\right]$$

$$U_3\equiv\frac{\varrho}{2}\left[(6u-1)G_1-(2-6u)G_2+2uG_6\right]$$

$$S_G=\tfrac{1}{2}\,(G_1+G_2)+\tfrac{1}{6}\,G_6$$

$$S_{AB}=\tfrac{1}{2}\,(A_1+B_1+A_2+B_2)+\tfrac{1}{3}\,A_6$$

$$\varrho=a\cdot\cos\theta,\ \tau=a\cdot\sin\theta,\ v_a=3\sqrt{3}\cdot a^3\cdot\sin^2\theta\cdot\cos\theta/2.$$

$$a_4=t_4,\ b_4=\sin^2\theta\cdot l_4+t_4,\quad g_4=\cos^2\theta\cdot l_4+t_4,\ d_4=-\sin\theta\cdot\cos\theta\cdot l_4$$

$$M\omega^2(\Gamma^1)=-6(G_1+G_2)-2G_6 \tag{B7}$$

$$M\omega^2(\Gamma^5)=-3(A_1+B_1+A_2+B_2)-2A_6 \tag{B8}$$

$$M\omega^2(T^5)=-3(A_2+B_2)-2A_6-6(a_4+b_4) \tag{B9}$$

$$M[\omega^2(T^6)-\omega^2(T^5)]=-3(A_1+B_1)+3(A_2+B_2)+2A_6 \tag{B10}$$

$$M\omega^2(T^1)=-6G_2-2G_6-12g_4 \tag{B11}$$

$$M[\omega^2(T^3)-\omega^2(T^1)] = -6G_1+6G_2+2G_6 \tag{B12}$$

$$(6u-1)^2(A_1+B_1)+(2-6u)^2(A_2+B_2)+24u^2A_6+2(a_4+b_4)-\operatorname{tg}^2\theta(G_1+G_2+6g_3+2g_4) = 0 \tag{B13}$$

$$(6u-1)(A_1+B_1)-(2-6u)(A_2+B_2)+4uA_6-\operatorname{tg}\theta(D_1-D_2) = 0 \tag{B14}$$

$$(6u-1)(A_1-B_1)+(2-6u)(A_2-B_2)-2(a_4-b_4)+\operatorname{tg}\theta\,(D_1+D_2+2d_4) = 0 \tag{B15}$$

$$M\omega^2(X^2) = -2(A_1+A_2+A_6+a_3+a_4)-6(b_3+b_4) \tag{B16}$$

$$M\omega^2(X^3) = -A_1-3B_1-A_2-3B_2-2a_3-6b_3-2a_4-6b_4. \tag{B17}$$

We also used two equations for the frequencies of acoustic modes with polarization vectors in the mirror plane, at the point L of the Brillouin zone. For the upper (L^1) and lower (L^4) frequencies one has:

$$M\omega^2(L^1) = \tfrac{1}{2}(D^+_{22}+D^+_{33}-((D^+_{22}-D^+_{33})^2+4(D^+_{23})^2)^{\frac{1}{2}}) \tag{B18}$$

$$M\omega^2(L^4) = \tfrac{1}{2}(D^-_{22}+D^-_{33}-((D^-_{22}-D^-_{33})^2+4(D^-_{23})^2)^{\frac{1}{2}}) \tag{B19}$$

where:

$$D^{\pm}_{\alpha\beta} \equiv D_{\alpha\beta}\begin{pmatrix}L\\11\end{pmatrix} \pm D_{\alpha\beta}\begin{pmatrix}L\\12\end{pmatrix}$$

$$D_{22}\begin{pmatrix}L\\11\end{pmatrix} \equiv -\tfrac{3}{2}(A_1+B_1+A_2+B_2)-A_6-6a_3-2b_3-4b_4$$

$$D_{22}\begin{pmatrix}L\\12\end{pmatrix} \equiv \tfrac{1}{2}(3A_1-B_1-3A_2+B_2+2A_6)$$

$$D_{33}\begin{pmatrix}L\\11\end{pmatrix} \equiv -3(G_1+G_2)-G_6-8g_3-4g_4$$

$$D_{33}\begin{pmatrix}L\\12\end{pmatrix} \equiv G_1-G_2+G_6$$

$$D_{23}\begin{pmatrix}L\\11\end{pmatrix} \equiv -4d_4$$

$$D_{23}\begin{pmatrix}L\\12\end{pmatrix} \equiv -2D_1+2D_2.$$

The above formulas follow from the factorization of dynamical matrix at point L $(0, 1/(3\tau), -1/(6\varrho))$, (classification according to [2]).

To solve the system of equations in the algebraic approach AA, one has to combine first Eqs (B8), (B9), (B10) to obtain the quadratic equation for A_2+B_2 from (B6), and symmetrically, Eqs (B7), (B11), (B12), to obtain from (B5) the quadratic equation for G_6. Now, after calculating U_1 and U_3, one obtains the linearized (B3). Proceeding in this way, one finds 4 equivalent solutions consisting each of 15 force constants of the model.

REFERENCES

[1] H. Jones, *The Theory of Brillouin Zones and Electronic States in Crystals*, North-Holland Publ. Company, Amsterdam 1960.

[2] S. H. Koenig, A. A. Lopez, D. B. Smith, J. L. Yarnell, *Phys. Rev. Letters*, **20**, 48 (1968).

[3] L. A. Fal'kovskii, *Uspekhi Fiz. Nauk*, **94**, 1 (1968).

[4] J. L. Yarnell, J. L. Warren, R. G. Wenzel, S. H. Koenig, *IBM J. Res. Dev.*, **8**, 234 (1964).

[5] D. Smith, *Thesis*, New Mexico Univ., 1967, unpublished.

[6] J. Sosnowski, S. Bednarski, A. Czachor, *Neutron Inelastic Scattering*, IAEA Vienna, **1**, 157 (1958); J. Sosnowski, *Thesis*, INR Warsaw, 1968, unpublished.

[7] R. Fouret, *Ann. Phys.* (France), **8**, 611 (1963).

[8] E. G. Borvman, *Preprint Instituta Atomnoi Energii*. 1456, Moskva 1967.

[9] A. A. Maradudin, E. W. Montrol, G. H. Weiss, *Solid State Phys. Supplement*, **3** (1963).

[10] G. Leibfried, *Handbuch der Physik*, Band VII, Teil 2.

[11] A. Czachor, *Inelastic Scattering of Neutrons*, IAEA Vienna, **1**, 181 (1965).

[12] A. D. Woods, B. N. Brockhouse, R. A. Cowley, W. Cochran, *Phys. Rev.*, **131**, 1025 (1963).

[13] G. Gilat, G. Dolling, *Phys. Letters*, **157**, 586 (1967).

[14] B. A. Kotov, N. M. Okunieva, A. Plachenova, *Fiz. Tverdogo Tela*, **11**, 2003 (1969).

[15] D. Schiferl, C. S. Barret, *J. Appl. Phys.*, **2**, 30 (1969).

[16] A. de Bretteville, E. R. Cohen, A. D. Ballato, I. N. Greenberg, S. Epstein, *Phys. Rev.*, **148**, 575 (1966).

[17] R. E. Macfarlane, *Preprint of the Los Alamos Scientific Lab.* We are grateful to dr Macfarlane for making available to us the preprint of his paper prior to publication.

[18] R. I. Sharp, E. Warming, *J. Phys. F.* (*Metal Phys.*), **1**, 570 (1971).

[19] A. Czachor, *Phys. Status Solidi*, **54**, K65 (1972).